Molecular Crystals and Liquid Crystals
Publication details, including instructions for authors and subscription information:
http://www.tandfonline.com/loi/gmcl20

The Effect of Chromium and Aluminium Ion Substitution on Phase Analysis, Microstructure and Magnetic Properties of Sr-Hexaferrite Ceramics and Nanopowders Synthesized by the Auto Combustion Route

Mehrdad Shaygan [a], Amir Abbas Nourbakhsh [b], Morteza Mozafari [c], Mohsen Shahshahan [b] & Mohsen Nourbakhsh [d]

[a] Department of Material Science and Engineering, Najafabad branch, Islamic Azad University, Najafabad, Isfahan, Iran

[b] Department of Ceramic Engineering, Shahreza branch, Islamic Azad University, Shahreza, Isfahan, Iran

[c] Physics Department, Razi University, TaghBostan, Kermanshah, Iran

[d] R&D Department, Taban Magnetic material development Co., Isfahan, Iran

Available online: 14 Feb 2012

To cite this article: Mehrdad Shaygan, Amir Abbas Nourbakhsh, Morteza Mozafari, Mohsen Shahshahan & Mohsen Nourbakhsh (2012): The Effect of Chromium and Aluminium Ion Substitution on Phase Analysis, Microstructure and Magnetic Properties of Sr-Hexaferrite Ceramics and Nanopowders Synthesized by the Auto Combustion Route, Molecular Crystals and Liquid Crystals, 555:1, 94-103

To link to this article: http://dx.doi.org/10.1080/15421406.2012.634755

Mol. Cryst. Liq. Cryst., Vol. 555: pp. 94–103, 2012

ISSN: 1542-1406 print/1563-5287 online
DOI: 10.1080/15421406.2012.634755

Taylor & Francis
Taylor & Francis Group

The Effect of Chromium and Aluminium Ion Substitution on Phase Analysis, Microstructure and Magnetic Properties of Sr-Hexaferrite Ceramics and Nanopowders Synthesized by the Auto Combustion Route

MEHRDAD SHAYGAN,[1] AMIR ABBAS NOURBAKHSH,[2,*] MORTEZA MOZAFARI,[3] MOHSEN SHAHSHAHAN,[2] AND MOHSEN NOURBAKHSH[4]

[1]Department of Material Science and Engineering, Najafabad branch, Islamic Azad University, Najafabad, Isfahan, Iran
[2]Department of Ceramic Engineering, Shahreza branch, Islamic Azad University, Shahreza, Isfahan, Iran
[3]Physics Department, Razi University, TaghBostan, Kermanshah, Iran
[4]R&D Department, Taban Magnetic material development Co., Isfahan, Iran

The chromium and aluminium quantitiesrequired to synthesize nano-sized $SrCr_xFe_{12-x}O_{19}$ and $SrAl_xFe_{12-x}O_{19}$ by the auto combustion route were optimized. XRD analysis showed that the optimum amounts were differed in two cases. A combination of 0.75 wt% of nano-sized $SrFe_{12}O_{19}$ and 0.75 wt% of the commercial additive, in chromium doped sample from solid state process(Cr_2O_3 addition), resulted in superior magnetic properties with increased intrinsic coercivity, remanence magnetization and rectangularity ratio.

Keywords Auto combustion route; ion substitution; strontium hexaferrite

Introduction

Hexagonal hard ferrites with magnetoplumbitestructure such as $SrFe_{12}O_{19}$ are applicable in many fields such as permanent magnets, high density recording medias, telecommunications, magneto optical and microwave devices [1]. M-type hexaferrites owed their extensive applications to their prominent properties such as high Curie temperature, high coercive force, high magnetic anisotropy field, excellent chemical stability and corrosion resistivity [2]. Alabanese et al. [3] showed that in cationic-substituted M-type hexagonal ferrites, the distribution of metallic ions among the differentsublattices greatly modified by replacement of Ba with Sr. In this regard, studies are mainly concentrated on transition-metal substitution, for example, Ga^{3+}, Ti^{4+}, Al^{3+}, Zn^{2+}, Co^{2+}, Cr^{3+}, La^{3+}, Pr^{3+}, Ce^{3+} and Zr^{2+} - Mn^{2+} to substitute Fe^{+3} ions of hexaferrite [4–8]. In a previous study, the optimum amount

*Address correspondence to Amir Abbas Nourbakhsh, Department of Ceramic Engineering, Shahreza branch, Islamic Azad University, Shahreza, Isfahan, Iran. E-mail: nourbakhsh@iaush.ac.ir

of Cr^{3+} content in chromium doped strontium hexaferrite was determined at 0.3 atom% Cr^{3+} content; higher Cr contents led to the appearance of non-magnetic hematite [9]. In order to achieve highly homogenous particles of strontium and barium hexaferrite, various techniques such as chemical co-precipitation [10], hydrothermal [11], sol-gel [12,13] and glass crystallization [14] have been developed. Conventional solid state method, as the classical ceramic rout for preparing strontium hexaferrite, requires a high calcining temperature (1200–1300°C) which induces in sintering and aggregation of particles. Furthermore, the milling process used to reduce the particle size from multi domain to single domain, generally yields non-homogeneous mixtures on a microscopic scale and results in lattice strain in the materials [15]. Recently, the sol–gel auto-combustion (citrate-nitrate), as a novel process, based on the gelling and subsequent combustion of an aqueous solution containing salts of the desired metals and some organic fuels, has given a voluminous and fluffy product with large surface area [2].

In the present study, the chromium and aluminium amounts to synthesize nano-sized $SrCr_xFe_{12-x}O_{19}$ and $SrAl_xFe_{12-x}O_{19}$ from auto combustion routewere optimized. Results of XRD analysis showed that the optimized amounts were different in two cases. A combination of 0.75 wt% of nano-sized $SrFe_{12}O_{19}$ and 0.75 wt% of the commercial additive, in chromium doped sample from solid state process(Cr_2O_3 addition), increased the intrinsic coercivity, remanence magnetization and rectangularity ratio and result in superior magnetic properties.

Experimental

The starting materials used to synthesis the nanostructured $SrCr_xFe_{12-x}O_{19}$ and $SrAl_xFe_{12-x}O_{19}$ were iron nitrate, strontium nitrate, chromium nitrate, aluminium nitrate, citric acid and ammonia, all of them having analytic purity. Appropriate amounts of $Fe(NO_3)_3.9H_2O$, $Sr(NO_3)$, $Cr(NO_3)$ and $Al(NO_3)$, considering different molar ratios, were dissolved in minimum amount of deionized water. Citric acid then added into the prepared aqueous solution to chelate Sr^{+2} and Fe^{+3} in the solution. The mixed solution neutralized to pH7 by adding liquor ammonia. The solution evaporated to dryness by heating at 100°C on a hot plate with continuous stirring until the mixture formed a viscous brown gel, which then calcined in air at different temperatures up to 1100°C for 1 hr.

In previous study, the optimum conditions for the development of the magnetic properties of chromium doped strontium hexaferrite were determined as 1220°C with 0.3 atom% Cr^{3+} content [9]. Before firing these powder mixtures, 1.5 wt% of nano-sized $SrFe_{12}O_{19}$ prepared, as described before, was added as a sintering aid, and for comparison, some samples were prepared with 1.5 wt% of a commercial calcium silicate borate sintering aid (Type MN112 Taban Magnetic material development Co, Iran). Three types of samples were prepared, one containing only the commercial additive, one containing only the nano-sized $SrFe_{12}O_{19}$ and one containing 0.75 wt% of each additive. Aqueous slurries of these powder mixtures were blended in steel jars for 8 h in the ball: water:powder ratio of 11:3:1. The slurries were then pressed under a magnetic field of 400–800 $A.m^{-1}$ at a pressure of 100 MPa to form pellets 3 cm in diameterand 1 cm thick and fired in air at 1210–1260°C for 2 h at a heatingrate of 10°C/min.

The XRD patterns of the products were determined using a BruckerD8diffractometer with Cu-Kα radiationand a Ni filter.FE-SEM studies carried out, after coating with Au, using a Hitachi S4160 electron microscope operated at 20 KeV. The magnetic properties of all the samples were determined by measuring their hysteresis loops using a model AMT-4 magnetometer (Shuangji Electronic Co, China).

Results and Discussion

Optimization of Calcining Temperature for Undopednano-Sized $SrFe_{12}O_{19}$

The synthesis of nano-sized $SrFe_{12}O_{19}$ powder by citrate-nitrate route is controlled by the ratio of Fe:Sr, the ratio of citrate to the other metal ions and the pH of the system. To obtain monophase $SrFe_{12}O_{19}$, the ratio of citrate ion to the metal ions was set at 1, with the pH of about 7. The XRD diffraction patterns of the unfired product and samples fired at 700 and 1100°C (Fig. 1) show that the optimal calcining temperature is about 1100°C. By increasing calcining temperature, the non-magnetic phase (hematite) was disappeared.Higher temperatures than 1100°C result to grain growth during calcination and the grain size increase, which is not suitable to obtain higher amount of coercivity force in magnetic ceramics.

The Effect of Aluminium Doping on Nano-Sizedsr-Hexaferrite

Figure 2 shows powder diffraction patterns of aluminium substituted strontium hexaferrite samples where $x = 0.5$, 2.5 and 4.5. The Figure shows that non-magnetic phase (α-Fe_2O_3) appeared in all sample. Because the radius of Al^{3+}, 0.54 Å, is almost smaller than Fe^{3+} ion, 0.64 Å, substitution of Al^{3+} instead of Fe^{3+} could be easier. Also, the change in the exchange energy after Al^{3+} ion substitution and the position of aluminium ion in hexaferrite structure could be responsible for hematite appearance as a non-magnetic phase. Mossbauer studies indicate that the hexagonal cell of $SrFe_{l2}O_{l9}$ contains five distinguishable crystallographic Fe sites; three octahedral 12k, $4f_2$ and 2a, one tetrahedral $4f_1$ and one bi-pyramidal 2b site, whereas only 82% of Al^{3+} exist in b-sub lattice (site 2a) and 18% of Al^{3+} ions are statistically distributed in the other sub lattices for $SrAl_xFe_{12-x}O_{19}$ [16].

Figure 3 shows the FE-SEM micrographs of Al-doped strontium hexaferritenanopowderscalcined at 1100°C for 5 h. Plate-like and hexagonal shaped Sr-hexaferrite are observed. These results show that Al-doped strontium hexaferritenanopowder is not suitable as an additive to $SrFe_{12}O_{19}$ bodies due to appearances of non-magnetic phase (α-Fe_2O_3).

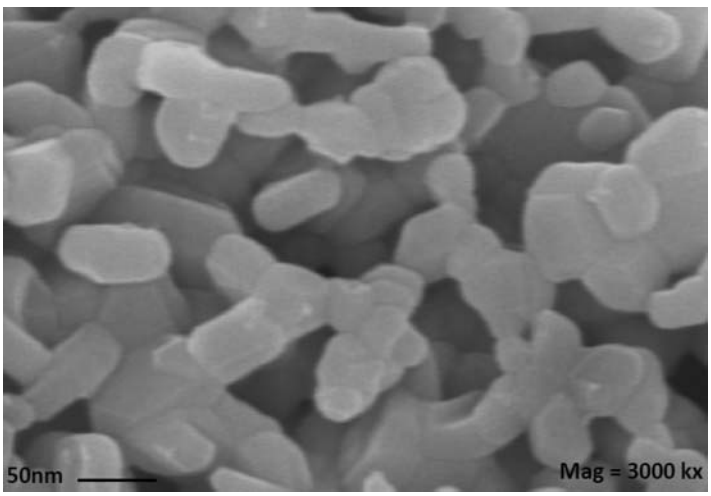

Figure 1. FE-SEM micrograph of nano-sized strontium hexaferrite.

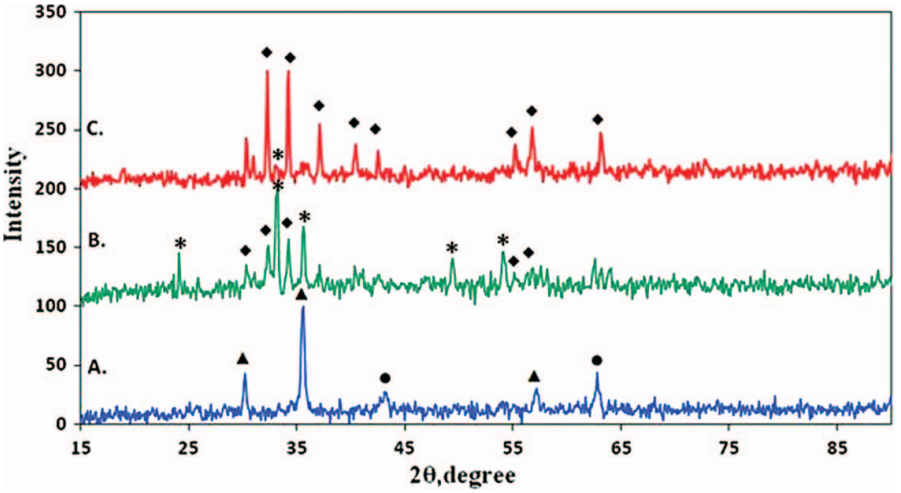

Figure 2. XRD patterns of nano-sized $SrFe_{12}O_{19}$ prepared by the citrate-nitrate method. A. As-synthesised, B. Calcined at 700°C, C. Calcined at 1100°C. Peaks marked * are from hematite (JCPDS file no: 33-0664), peaks marked ♦ are from $SrFe_{12}O_{19}$ (JCPDS file no: 33-1340), peaks marked • are from maghemite (JCPDS file no: 39-1346) and peaks marked ▲ are from magnetite (JCPDS file no: 19-0629).

The Effect of Chromium Doping on Nano-Sizedsr-Hexaferrite

XRD patterns of nano-sized Cr-doped $SrCr_xFe_{12-x}O_{19}$ where x = 0.1–0.7 showed no change up to x = 0.4 atom% Cr^{3+} (Fig. 4). The non-magnetic phase (hematite) was appeared at higher amount than x = 0.4 atom% Cr^{3+}. According to FE-SEM micrographs, which are

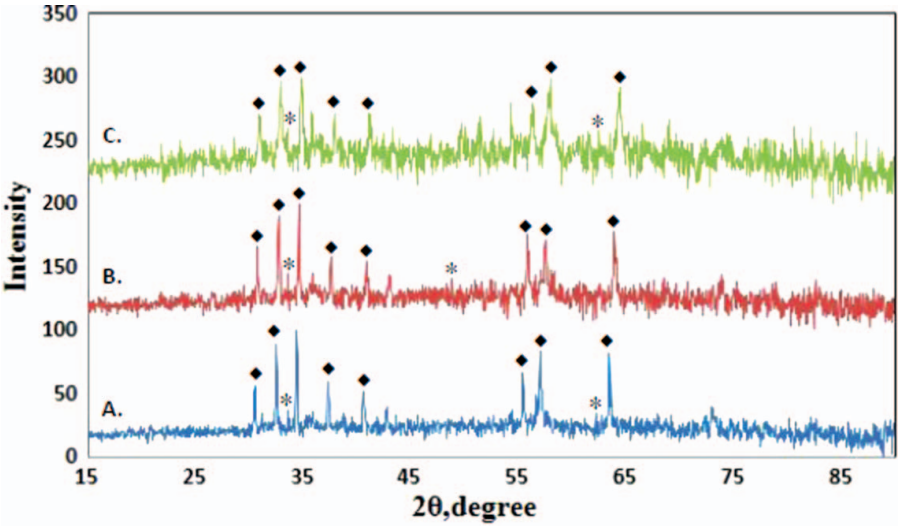

Figure 3. XRD patterns of aluminium substituted strontium hexaferrite ($SrAl_xFe_{12-x}O_{19}$) prepared by the citrate-nitrate route. A. x = 0.5, B. x = 2.5, C. x = 4.5. Peaks marked * are from hematite (JCPDS file no: 33-0664), peaks marked ♦ are from SrFe12O19 (JCPDS file no: 33-1340).

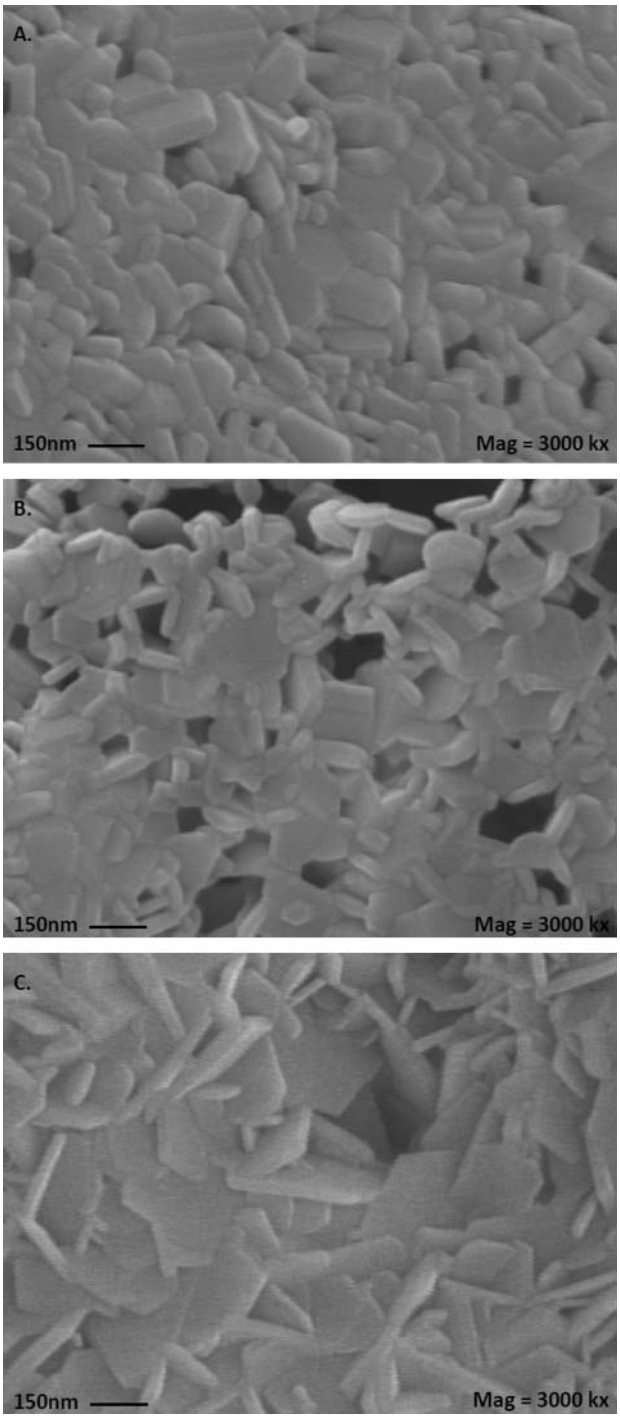

Figure 4. FE-SEM micrographs of Al-doped strontium hexaferrite nanopowders calcined at 1100°C for 5 h. A. x = 0.5, B. x = 2.5, C. x = 4.5.

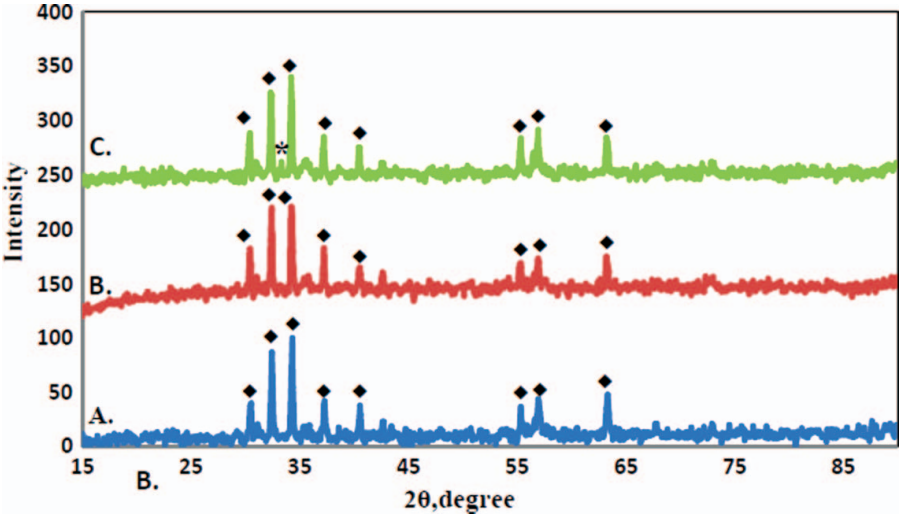

Figure 5. XRD patterns of chromium substituted strontium hexaferrite ($SrCr_xFe_{12-x}O_{19}$) prepared by the citrate-nitrate route. A. x = 0.1, B. x = 0.4, C. x = 0.7. Peaks marked * are from hematite (JCPDS file no: 33-0664), peaks marked ♦ are from $SrFe_{12}O_{19}$ (JCPDS file no: 33-1340).

shown in Fig. 5 and EDS analysis (not shown here) hematite, as a non-magnetic phase, could be distinguished by white particles showed good correspondence to XRD analysis results. The average size of nano-sized Cr-doped $SrCr_xFe_{12-x}O_{19}$ with various amounts of chromium, 0.1, 0.4 and 0.7, which fired at 1100°C were about305 nm, 85 nm and 210 nm, respectively. These results could be related to nucleation and growth mechanism in chromium-doped samples.

Development of Magnetic Properties of Sr-Hexaferrite by Addition of $SrFe_{12}O_{19}$ nanopowder

XRD patterns studies of Cr-doped $SrCr_xFe_{12-x}O_{19}$ samples, where x = 0-0.5, show no change up to x = 0.3, but at x = 0.5 the non-magnetic hematite phase appears [9]. In general, Cr atoms do not occupy tetrahedralsites, ruling out substitution in the $4f_1$ siteand confiningthe substitution to 10 of the 12 Fe^{3+} ions in $SrFe_{12}O_{19}$ [17]. Since the ionic radius of Cr^{+3} and Fe^{+3} are almost equal, the appearance of hematite is unlikely to result from the effect of size but may be due to the change of exchange energy accompanying Cr^{3+} substitution in the lattice [8].

The magnetic properties of Cr-doped $SrCr_xFe_{12-x}O_{19}$ sintered at various temperatures in the presence of 1. 5 wt% MN112 sintering additive are shown in Fig. 6, as a function of Cr content. Increasing the amount of chromium up to x = 0.5, results in a decrease of remanence magnetization at all temperatures. This may be related to the electron configuration of Cr^{3+}, which results in a magnetization of $3\mu B$, whereas Fe^{3+} is $5\mu B$. These results suggest that a Cr doping content of x = 0.3 produced a product with optimal magnetic properties, and this composition was adopted for the subsequent studies of the effect of nano-sized $SrFe_{12}O_{19}$ additive.

Because attempt of the Cr^{3+} ion substitution in $SrFe_{12}O_{19}$ lattice structure showed limit solubility, the addition of nano-sized strontium hexaferrite without chromium was selected

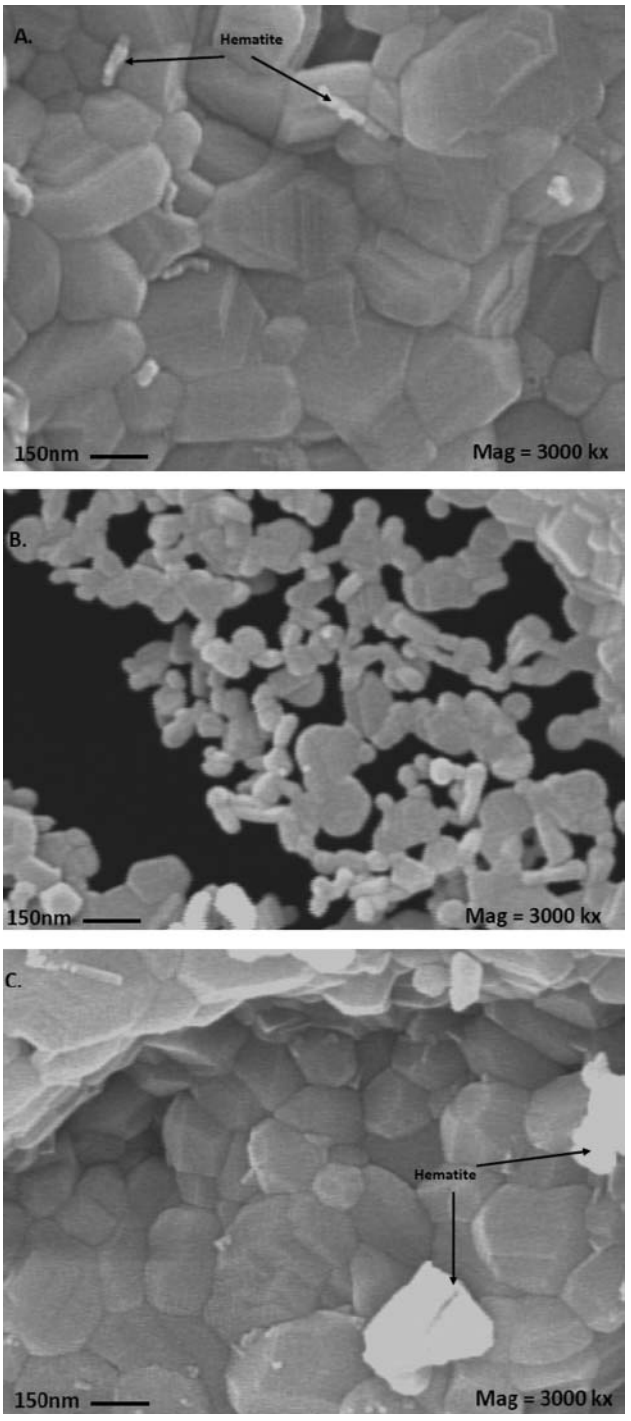

Figure 6. FE-SEM micrographs of Cr-doped strontium hexaferrite nanopowders calcined at 1100°C for 5 hrs. A. x = 0.1, B. x = 0.4, C. x = 0.7.

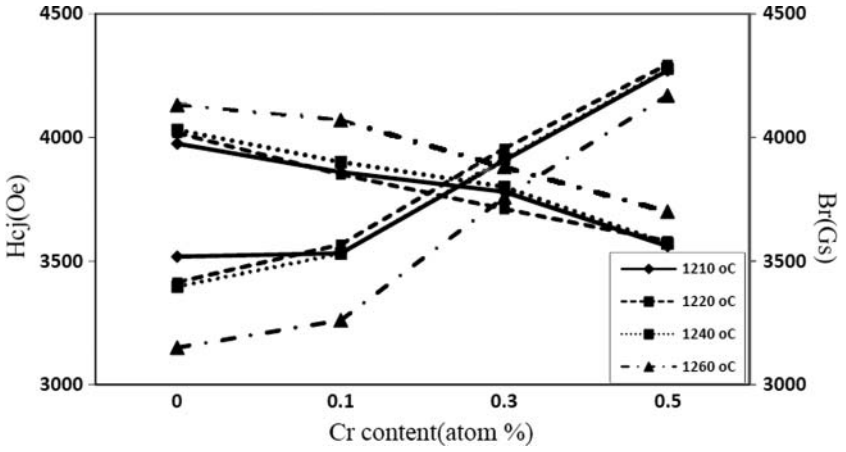

Figure 7. Remanence Magnetization and Coercive field of Cr-doped $SrFe_{12}O_{19}$ sintered with 1.5 wt% MN112 sintering additive as a function of Cr content.

during solid state process using Cr_2O_3. Table 1 compares the magnetic properties of the initial $SrFe_{12}O_{19}$ powder, the sintered product doped with the optimal 0.3 mole Cr, and this doped material sintered with 1.5 wt% of nano-sized $SrFe_{12}O_{19}$, with the results for the sample containing 1.5 wt% sintering additive for comparison. Table 1 shows that sintering $SrCr_{0.3}Fe_{11.7}O_{19}$ with nano-sized $SrFe_{12}O_{19}$ additive alone produced little difference in remanence magnetization from the sample sintered without any additives, but the coercive field is significantly decreased by the presence of the nano-additive. The use of MN112 sintering additive decreased the remanence magnetization of undoped $SrCr_{0.3}Fe_{11.7}O_{19}$ but significantly increases the coercive field; this effect is even more pronounced in the sample containing equal proportions of MN112 and nano-$SrFe_{12}O_{19}$ (Table1), indicating that this combination of additives produces the best practical magnetic material. The use of the two additives together combined the best properties of each, producing the sample with a superior coercive field and therefore the best magnetic properties for practical applications.

Table 1. Comparison of the magnetic properties of the various samples

Sample and firing temperature	Remanence Magnetization (G)	Coercive field (Oe)	Rectangularity ratio (%)
Undoped $SrFe_{12}O_{19}$ powder (1210°C)	3673	4048	87.1
$SrCr_{0.3}Fe_{11.7}O_{19}$ (no additive, sintered 1220°C)	3806	2941	76.9
$SrCr_{0.3}Fe_{11.7}O_{19}$ +1.5 wt% nano-$SrFe_{12}O_{19}$ (sintered 1220°C)	3888	2525	91
$SrCr_{0.3}Fe_{11.7}O_{19}$ + 1.5 wt% MN112 (sintered 1220°C)	3662	3928	70
$SrCr_{0.3}Fe_{11.7}O_{19}$ + 0.75 wt% nano-$SrFe_{12}O_{19}$ + 0.75 wt% MN112 (sintered 1220°C)	3687	4129	84

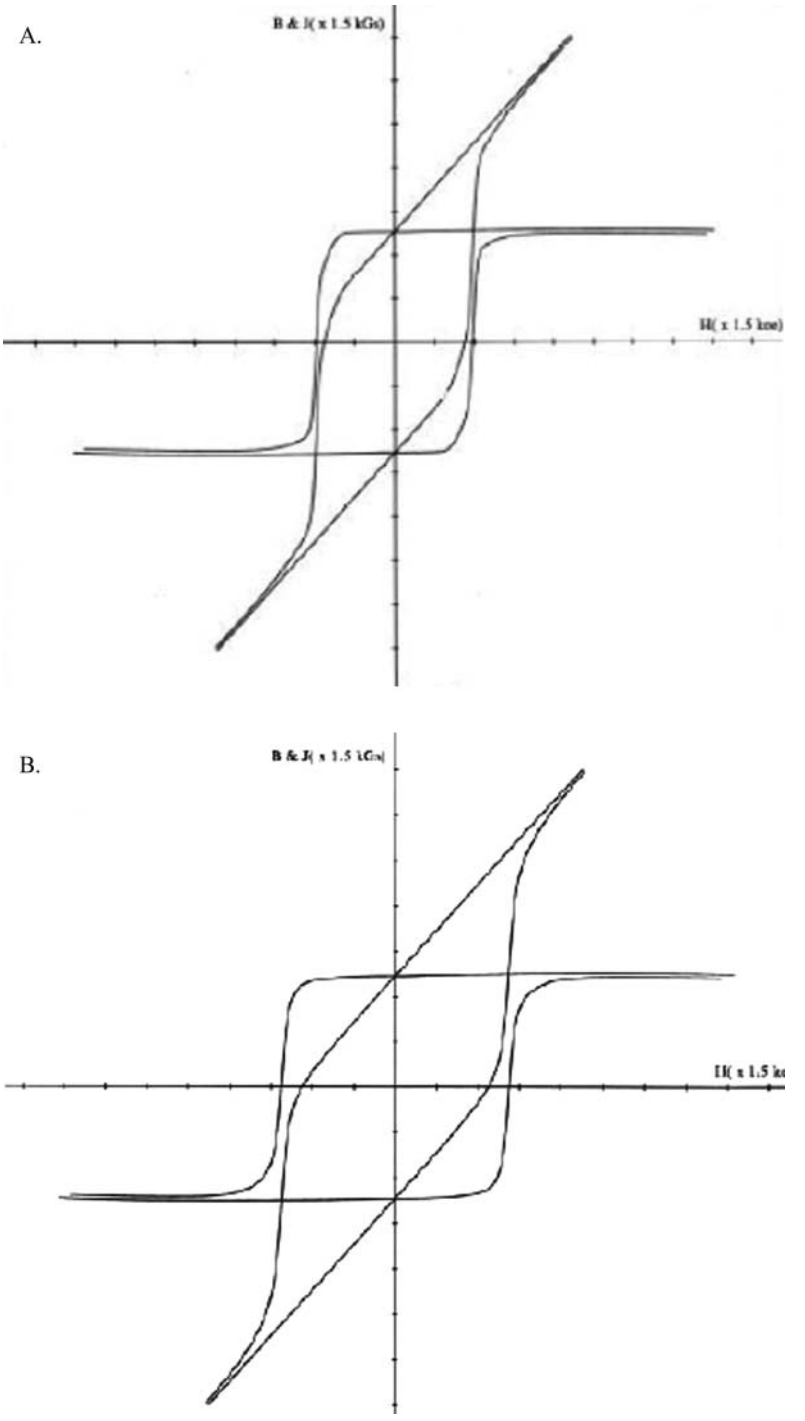

Figure 8. Hysteresis loop of optimized $SrCr_{0.3}Fe_{11.7}O_{19}$ sample, sintered at 1220°C. A. Before using additive, B. After using 0.75 wt% nano-sized $SrFe_{12}O_{19}$ + 0.75 wt% MN112 sintering additive.

Conclusions

Sample of chromium and aluminium doped strontium hexaferrite synthesized by auto combustion route. The calcining temperature and grain size of undoped nano-sized $SrFe_{12}O_{19}$ determined. Because of the existence of the non-magnetic phase (hematite)in all the samples of $SrAl_xFe_{12-x}O_{19}$, Al**-**doped strontium hexaferrite nanopowder is not suitable as an additive to $SrFe_{12}O_{19}$ bodies. Samples of $SrFe_{12}O_{19}$ were doped with 0.3 atom% Cr^{3+} and sintered with the addition of 1.5 wt% nano-sized $SrFe_{12}O_{19}$ in conjunction with a commercial calcium silicate borate sintering aid. The addition of nano-sized $SrFe_{12}O_{19}$ alone, leads to enhanced grain growth, with deleterious effects on the magnetic properties, particularly the important coercive field value, whereas the use of 1.5 wt% of commercial sintering additive alone promotes greater sintering with a significant enhancement of the coercive field. The combination of 0.75 wt% of each additive produces the best magnetic properties in these Cr-doped samples (a remanence magnetization of 3687 G, a coercive field of 4129 Oe and a rectangularity ratio of 84%).

References

[1] Iqbal, M. J., Ashiq, M. N., Hernandez, P., & Munoz, J. M. (2008). *J. Magn. Magn. Mater.*, *320*, 881.
[2] Mali, A., & Ataie, A. (2004). *Ceramic International*, *30*, 1979–1983.
[3] Albanese, G., Carbucicchio, M., & Deriu, A. (1973). *J. Sol. Stat. Phys.*, *15*, 147.
[4] You, L. Q., & Zheng, J. (2007). *J. Magn. Magn. Mater.*, *318*, 74.
[5] Wang, J. F., Ponton, C. B., & Harris, J. R. (2005). *J. Alloys Compd.*, *403*, 10.
[6] Martirosyan, K. S., Martirosyan, N. M., & Chalykh, A. E. (2004). *Inorganic Mater.*, *40*, 527.
[7] Iqbal, M. J., & Ashiiq, M. N. (2007). *Scripta Mater.*, *56*, 14.
[8] Fang, Q., Cheng, H., Huang, K., Wang, J., & Li, R. (2005). *J. Magn. Magn. Mater.*, *294*(3), 281.
[9] Nourbakhsh, A. A., Nourbakhsh, M., Shaygan, M., & Mackenzie, K. J. D. (in Press). *J. Mater. Sci. Material in Electronics*.
[10] Ataei, A., & Heshmati-Manesh, S. (2001). *J. European Ceramic Soc.*, *21*, 1951.
[11] Wang, J. F., Paton, C. B., Ciossinger, R., & Harris, I. R. (2004). *J. Alloys and Compd.*, *369*, 170.
[12] Jotania, R. B., Khomane, B. B., Chauhan, C. C., Menon, S. K., & Kulkari, B. D. (2002). *J. Magn. Magn. Mater.*, *310*, 2477.
[13] Junliang, L., Yanwei, Z., Cuijing, C., Wei, Z., & Xiaowei, Y. (2010). *J. Eur. Ceram. Soc.*, *30*, 993.
[14] Mirkazemi, M., Marghusiiam, V. K., & Beitollahi, A. (2006). *Ceramic Internat.*, *32*, 43.
[15] Kingery, W. D. et al. (1976). Introduction to Ceramics, John Wiley and Sons Inc.
[16] Eraky, M. R., Beslepkin, A. A., & Kuntesvich, S. P. (2003). *Mater. Lett.*, *57*, 3427.
[17] Rao, P. M., Rard, G., & Grandjea, P. (1979). *Phys. Stat. Sol.*, *54*, 529.
[18] Goldman, A. (1990). Modern Ferrite Technology, New York: Nostrand Reinhold.
[19] Arendt, R. H. (1973). *J. Appl. Phys.*, *44*, 330.